ARTICLE

OBC
www.rsc.org/obc

Overcrowded 1,8-diazafluorenylidene-chalcoxanthenes. Introducing nitrogens at the fjord regions of bistricyclic aromatic enes

Amalia Levy, Shmuel Cohen and Israel Agranat*
Department of Organic Chemistry, The Hebrew University of Jerusalem, Jerusalem 91904, Israel. E-mail: isria@vms.huji.ac.il

Received 20th March 2003, Accepted 11th June 2003
First published as an Advance Article on the web 30th June 2003

The effects of introducing nitrogen atoms in the fjord regions and chalcogen bridges on the conformations of overcrowded bistricyclic aromatic enes (**1**, X ≠ Y) (BAEs) were studied. 9-(9′*H*-1′,8′-Diazafluoren-9′-ylidene)-9*H*-thioxanthene (**12**), 9-(9*H*-1′, 8′-diazafluoren-9′-ylidene)-9*H*-selenoxanthene (**13**), 9-(9′*H*-1′,8′-diazafluoren-9′-ylidene)-9*H*-telluroxanthene (**14**), 9-(9′*H*-1′,8′-fluoren-9-ylidene)-9*H*-xanthene (**15**) and 9-(9′*H*-1′,8′-fluoren-9′-ylidene)-9*H*-fluorene (**16**) were synthesized by two-fold extrusion coupling reactions of 1,8-diaza-9*H*-fluoren-9-one (**19**)/chalcoxanthenthiones (**24**–**27**) (or /9*H*-fluorene-9-thione (**30**)). The 1′,8′-diazafluoren-9-ylidene-chalcoxanthenes (**11**) were compared with the respective fluoren-9-ylidene-chalcoxanthenes (**10**). The structures of **12**–**16** were established by ^{1}H, ^{13}C, ^{77}Se, and ^{125}Te NMR spectroscopies. The crystal and molecular structures of **12**–**14** were determined by X-ray analysis. The yellow molecules of **12**–**14** adopted mono-folded conformations with folding dihedrals in the chalocoxanthylidene moieties of 62.7° (**12**), 62.4° (**13**) and 59.9° (**14**). The folding dihedrals in the respective 1′,8′-diazafluorenylidene moieties were very small, *ca.* 2°, compared with 10.2/8.0° in (9′*H*-fluoren-9′-ylidene)-9*H*-selenoxanthene (**7**). A 5° pure twist of $C^9{=}C^{9'}$ in **14** is noted. The degrees of overcrowding in the fjord regions of **12**–**14** (intramolecular non-bonding distances) were relatively small. The degrees of pyramidalization of C^9 and $C^{9'}$ were 17.0/3.0° (**12**), 17.4/2.4° (**13**) and 2.2/2.2° (**14**). These high values in **12** and **13** stem from the resistance of the 1,8-diazafluorenylidene moiety to fold and from the limits in the degrees of folding of the thioxanthylidene and selenoxanthylidene moieties (due to shorter S^{10}–C^{4a}/S^{10}–C^{10a} and Se^{10}–C^{4a}/Se^{10}–C^{10a} bonds, as compared with the respective Te–C bonds in **14**). The molecules of **15** and **16** adopt twisted conformations, a conclusion drawn from the ^{1}H NMR chemical shifts of the fjord regions protons (H^1 and H^8) at 8.70 (**15**) and 9.00 ppm (**16**) and from their colors and UV/VIS spectra: **15** is purple (λ_{max} = 521 nm) and **16** is orange–red. A comparison of the NMR spectra of **11** and **10** ($\Delta\delta = \delta(\mathbf{11}) - \delta(\mathbf{10})$) showed substantial downfield shifts of 0.56–0.62 ppm of the fjord regions protons of twisted **15** and **16**: $\Delta\delta$ (C^9) were negative (upfield): −4.0 (**12**), −3.7 (**13**), −3.4 (**14**), −7.1 (**15**), −5.0 ppm (**16**), while $\Delta\delta$ ($C^{9'}$) were positive (downfield) = +6.8 (**12**), +6.5 (**13**), +5.8 (**14**), +11.7 (**15**), +7.7 ppm (**16**). In **15**, $\Delta\delta$ (C^9) – $\Delta\delta$ ($C^{9'}$) = +18.8 ppm, attributed to a push–pull character and significant contributions of zwitterionic structures in the twisted conformation. The ^{77}Se and ^{125}Te NMR signals of **13** and **14** were shifted upfield relative to the respective fluorenylidene-chalcoxanthene derivatives: $\Delta\delta^{77}$Se = 17.2 ppm and $\Delta\delta^{125}$Te = 22.0 ppm. The presence of the nitrogen atoms ($N^{1'}$ and $N^{8'}$) in **13** and **14** causes shielding of the selenium and tellurium nuclei.

Introduction

The bistricyclic aromatic enes (BAEs) (**1**) have fascinated chemists since bifluorenylidene (**2**) and dixanthylene (**3**) were synthesized and thermochromism was revealed in bianthrone (**4**).[1–5] They can be classified into homomerous bistricyclic enes (**1**, X = Y) and heteromerous bistricyclic enes (**1**, X ≠ Y).[3,6] The BAEs are nonplanar and overcrowded in the fjord regions. There are two principal modes of out-of-plane deformations in **1**: twisting around the central double bond ($C^9{=}C^{9'}$) and out-of-plane bending,[3,4] realized by folding of the tricyclic moieties.[3,4,7] In addition, C^9 and $C^{9'}$ may be pyramidalized.[1–4] The nonplanarity of **1** may introduce chirality.[4,6] The major mode of deviation from planarity is dependent on the sizes of the central rings and on the bridges X, Y (bond lengths C–X and C–Y, distances $C^{4a} \cdots C^{10a}$).[3,8,9] A variety of conformations have been revealed in the homomerous bistricyclic enes, including twisted (**t**) bifluorenylidene[10,11] (**2**), *anti*-folded (**af**) dixanthylene[12] (**3**), *anti*-folded (**af**) bianthrone[13] (**4**), and *anti*-folded (**af**) and *syn*-folded (**sf**) 5,5′-bi(5*H*-dibenzo[*a*,*d*] cyclohepten-5-ylidene)[14] (**1**, X = Y = HC=CH).

We have recently described the syntheses and stereochemistry of homomerous and heteromerous selenium- and tellurium-bridged bistricyclic aromatic enes **5**–**8**. Homomerous 9,9′-bi(9*H*-selenoxanthen-9-ylidene) (**5**) and 9,9′-bi(9*H*-telluroxanthen-9-ylidene) (**6**) adopted *anti*-folded conformations with 53.6° (**5**) and 53.1° (**6**) folding dihedrals between pairs of benzene rings of the tricyclic moieties and showed low degrees

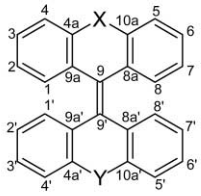

1, X=Y *homomerous*
1, X≠Y *heteromerous*

of overcrowding in the fjord regions.[15] Heteromerous 9-(9′*H*-fluoren-9′-ylidene)-9*H*-selenoxanthene (**7**) and 9-(9′*H*-fluoren-9′-ylidene)-9*H*-telluroxanthene (**8**), with central five-membered and six-membered rings, adopted the *anti*-folded and folded conformation with 56.3/62.0° and 10.2/8.0° (**7**) and 63.6° and 2.2° (**8**) folding dihedrals.[16] We have also reported on the interplay between twisting and folding in the conformational space of 9-(9′*H*-fluoren-9′-ylidene)-9*H*-xanthene (**9**).[17] These three systems belong to the fluorenylidene-chalcoxanthene (**10**, X: O, S, Se, Te) series. It seemed interesting to extend the above studies to heteromerous BAEs by introducing nitrogen atoms at the overcrowded fjord regions of **1**. For this purpose, we have studied the 1,8-diazafluorenylidene-chalcoxanthene (**11**, X: O, S, Se, Te) series. The present article describes the syntheses, molecular and crystal structures, and NMR spectra, of 9-(9′*H*-1′,8′-diazafluoren-9′-ylidene)-9*H*-thioxanthene (**12**), 9-(9′*H*-1′,8′-diazafluoren-9′-ylidene)-9*H*-selenoxanthene (**13**), 9-(9′*H*-

DOI: 10.1039/b303041e

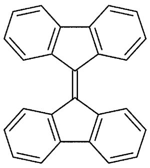
2

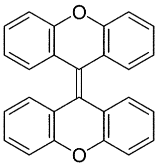
3

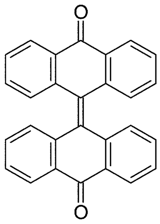
4

1′,8′-diazafluoren-9′-ylidene)-9*H*-telluroxanthene (**14**), 9-(9′*H*-1′,8′-diazafluoren-9′-ylidene)-9*H*-xanthene (**15**) and related derivatives. This series contains six-membered central rings with chalcogen bridges, five-membered central rings, and two nitrogens (instead of carbons) at the fjord regions (positions 1′ and 8′). For comparison, we have also studied 9-(9′*H*-1′,8′-diazafluoren-9′-ylidene)-9*H*-fluorene[18] (**16**), as a 1,8-diaza-derivative of bifluorenylidene (**2**), which was expected to be twisted. The van der Waals radius of nitrogen, 150 pm, is considerably shorter than that of carbon, 171 pm. This would render the fjord regions of **11** less overcrowded, as compared with **10**.[17] The fjord nitrogens of **11** may affect not only the overcrowding. One of the pertinent aspects of the conformational spaces of fluorenylidene-chalcoxanthenes (**10**) is their potential push–pull character, in which the fluorenylidene and the chalcoxanthylidene moieties may serve as an acceptor and a donor, respectively. The 1,8-diazofluorenylidene moiety may amplify this effect in **11** *versus* **10**. Furthermore, the energetic propensity of the fluorenylidene moiety against folding, contrary to the chalcoxanthylidene moieties, may be enhanced in the 1,8-diazafluorenylidene derivatives. The subtle balance between twisting and folding revealed in **9** may also be affected in the analogous **15**. We note the recent reports of the synthesis and crystal structure of the homomerous twisted 9,9′-bi-4,5-diazafluorenylidene[19] (**17**) and of a 4,5-diazafluorene-methoxybenzo[*a*]xanthene based overcrowded ene.[20] The synthesis of the homomerous 9,9′-bi(1,8-diazafluorenylidene) (**18**) has been reported.[18]

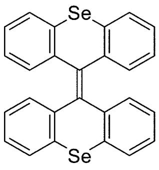
5

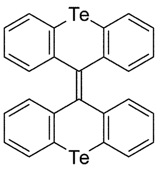
6

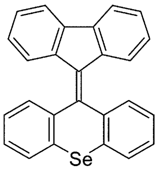
7

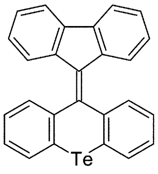
8

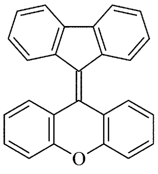
9

The 1,8-diazafluorenylidene functionality, which is at the core of the present study, is an inherent constituent of 9*H*-1,8-diazafluorenone (**19**) (DFO). DFO has proved to be the most important fluorogenic reagent in forensic investigations for the chemical development of latent fingerprints.[21–24] DFO reacts with α-amino acids to give a red dye which is highly fluorescent.

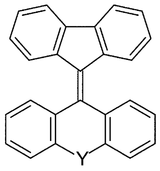
10 (Y= O, S, Se, Te)

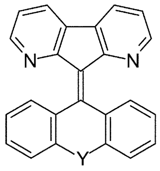
11 (Y= O, S, Se, Te)

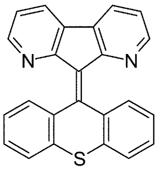
12

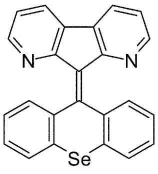
13

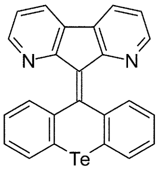
14

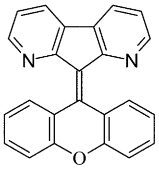
15

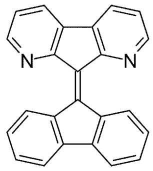
16

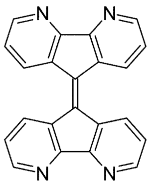
17

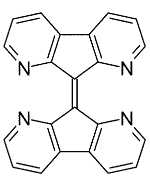
18

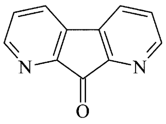
19

Synthesis

The 1′,8′-diazafluorenylidene-chalcoxanthenes **12**–**15** were synthesized by applying Barton's two-fold extrusion diazo–thione coupling method (Scheme 1).[25–27] In principle, both the diazo-1,8-diazafluorene–chalcoxanthenthione and the 1,8-diazafluorenthione–diazochalcoxanthene couplings could be adopted. The former route was preferred, taking advantage of the relatively convenient preparations of the reactants, their stabilities (aromatic dipolar structures) and their reactivities as carbon nucleophiles and carbon electrophiles, respectively, in the diazo–thione couplings. The method is especially suited for the synthesis of heteromerous bistricyclic enes. The starting materials for **12**–**15** were the tricyclic ketones 9*H*-thioxanthen-

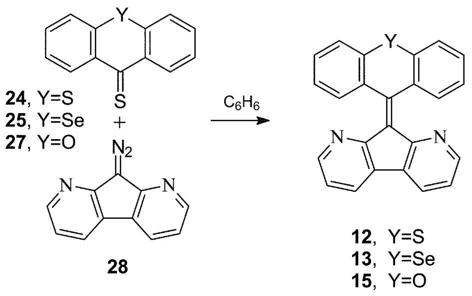

Scheme 1

9-one (**20**), 9*H*-selenoxanthen-9-one[28,29] (**21**), 9*H*-telluroxanthen-9-one[30,31] (**22**), 9*H*-xanthene-9-one (**23**), and 9*H*-1,8-diazafluoren-9-one (**19**). 9*H*-Thioxanthene-9-thione (**24**), 9*H*-selenoxanthene-9-thione (**25**), 9*H*-telluroxanthene-9-thione (**26**) and 9*H*-xanthene-9-thione (**27**) were prepared from **20**–**23**, respectively, using Lawesson's Reagent,[32–34] in boiling benzene, as previously described.[15] 9-Diazo-9*H*-1,8 diazafluorene[18] (**28**) was prepared from **19**[35,36] in two steps by conversion to the hydrazone **29**, followed by oxidation, using Ag$_2$O or HgO. The diazo–thione coupling of thione **24**, **25** and **27** and diazo **28** in boiling benzene gave directly the desired ethylenes **12**, **13**, and **15**, respectively, while the coupling between thione **26** and diazo **28** gave a mixture in a ratio 1 : 1 of **14** and the corresponding thiiran. The latter intermediate was not isolated. Reaction of this mixture with PPh$_3$ in benzene gave **14**. The known homomerous 9-(9′*H*-1,8-diazafluoren-9′-ylidene)-9*H*-fluorene[18] (**16**) was prepared by a coupling reaction between the diazo **28** and the 9*H*-flourene-9-thione[32] (**30**) in boiling benzene.

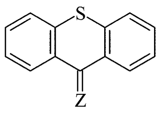

20, Z=O
24, Z=S

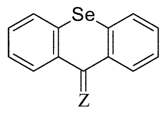

21, Z=O
25, Z=S

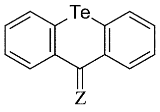

22, Z=O
26, Z=S

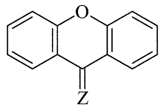

23, Z=O
27, Z=S

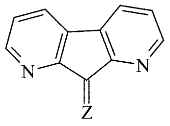

19, Z=O
28, Z=N$_2$
29, Z=NNH$_2$

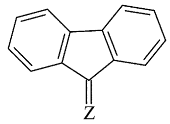

30, Z=S

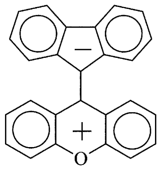

9a

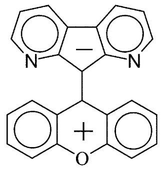

15a

Molecular and crystal structures

The crystal structures of bistricyclic aromatic enes (**1**) have been reviewed.[3] Recently we reported the molecular and crystal structures of the homomerous **5** and **6**[15] and the heteromerous **7** and **8**.[16] 9-(9′*H*-1′,8′-Diazafluoren-9′-ylidene)-9*H*-thioxanthene (**12**) and 9-(9′*H*-1′,8′ diazafluoren-9′-ylidene)-9*H*-selenoxanthene (**13**) crystallized in the space group *Pmn*2$_1$. Fig. 1 gives an ORTEP diagram of **13** as determined by X-ray analysis. In **12** and **13** the benzene rings are reflected through mirror planes that pass *via* the atoms S^{10}, C^9, C$^{9'}$ for **12** and Se^{10}, C^9, C$^{9'}$ for **13**. 9-(9′*H*-1′,8′-Diazafluoren-9′-ylidene)-9*H*-telluroxanthene (**14**) crystallized in the space group *P*21/*n*. Fig. 2 gives an ORTEP diagram of **14** as determined by X-ray analysis. Table 1 gives the conformations and selected geometrical parameters derived from crystal structures of **5**–**8** and **12**–**14**.

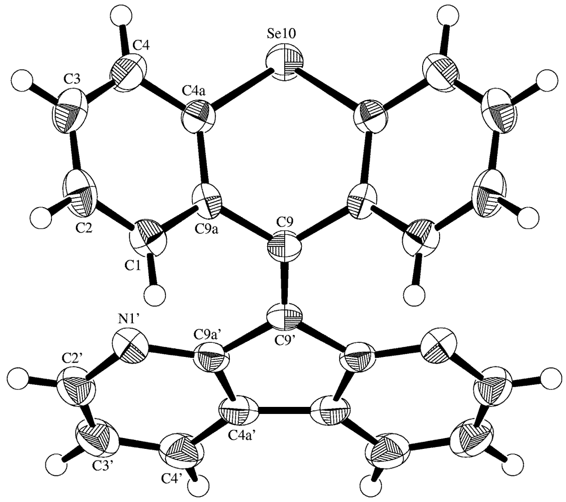

Fig. 1 ORTEP Diagram of the X-ray structure of **13**.

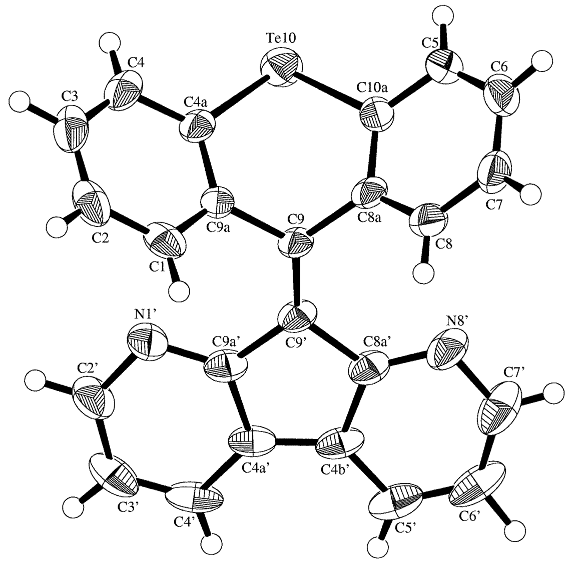

Fig. 2 ORTEP Diagram of the X-ray structure of **14**.

The overall conformations of the bistricyclic aromatic enes are characterized by the pure twist of the central C^9=C$^{9'}$ bond and by the folding dihedral of the tricyclic moieties. The folding dihedral is defined as the dihedral angle of the least-square-planes of the carbons C^1, C^2, C^3, C^4, C^{4a}, C^{9a} and C^5, C^6, C^7, C^8, C^{8a}, C^{10a} of the two benzene rings of a tricyclic moiety.[3] The pyramidalization angles χ_9 and $\chi_{9'}$ should also be considered.[3] The molecular and crystal structures of **12**–**14** indicated that they adopt (mono-) folded conformations (**f-12**, **f-13**, **f-14**). The folding dihedrals in the chalcoxanthenylidene moieties of **12**, **13** and **14** are 62.7°, 62.4°, and 57.9°, respectively. The folding dihedrals in the diazafluorenylidene moieties of **12**, **13** and **14** are very small, 1.5°, 1.8° and 2.1°, respectively. It is interesting to compare these data to the related systems **7** and **8**. There are two independent molecules of **7** in the unit cell, labeled **7a** and **7b**. The folding dihedrals in the fluorenylidene moieties of **7a** and **7b** are 10.2° and 8.0°, respectively. In the case of **8**, the folding dihedral in the fluorenylidene moiety is only 2.2°. The presence of the nitrogen atoms at the 1′, 8′ positions in the diazafluorenylidene moieties does not enhance the folding as it occurs in **7**. It would be expected that the folding dihedral in the telluroxanthenylidene moiety of **14** would at least be as high as in **8** (63.6°). However, the data showed that this folding dihedral is smaller, 57.9°. Furthermore, this folding dihedral is even smaller than that of the selenoxanthenylidene moiety in **7b** (62.0°). One explanation of this is the twist angle of 5° in **14**, which causes the Te^{10} ··· N^8 and Te^{10} ··· N^1 distances 539 pm

Table 1 Conformations and selected geometrical parameters of **5**–**8**, **12**–**14** derived from crystal structures and PM3 calculations

	Y	X	Method	[a]	Folding angle/°		Pure twist	$C^1\cdots N^{1'}$/pm	$C^8\cdots N^{8'}$/pm	$N^1\cdots H^{1'}$/pm	$N^8\cdots H^{8'}$/pm	$X^{10}\cdots N^{1'}$/pm	$X^{10}\cdots N^{8'}$/pm	$X^{10}\cdots C^{9'}$/pm
14	Te	—	X-ray	**f**	57.9	2.1	5.0	288	296	302	276	502	539	320
8	Te	—	X-ray	**f**	63.6	2.2	0.5	325	248	331			265	315
13	Se	—	X-ray	**f**	62.4	1.8	0.0	295	295	279	279	516	516	307
7a	Se	—	X-ray	**au**	56.3	10.2	0.7	307	240	297			255	308
7b	Se	—	X-ray	**au**	62.0	8.0	2.5	315	251	307			249	305
12	S	—	X-ray	**f**	62.7	1.5	0.0	290	290	258	258	517	517	306
6	Te	Te	X-ray	**af**	53.1	53.1	0.0	324	327	327			356	323
5	Se	Se	X-ray	**af**	52.5	54.7	1.6	326	319	319			348	308

[a] Conformation: **f**: folded; **au**: unevenly *anti*-folded.

	Y	X	Method	[a]	$C^9{=}C^{9'}$/pm	$C^{9a}–C^9–C^{8a}$/°		χ_9/°	$\chi_{9'}$/°	C–X/pm	C–X–C/°	$C^{4a}\cdots C^{10a}$/pm
14	Te	—	X-ray	**f**	135.2	113.1	103.8	2.2	2.2	212.2	88.8	295
8	Te	—	X-ray	**f**	135.0	111.0	105.0	8	15	212.4	88.1	295
13	Se	—	X-ray	**f**	134.9	111.5	104.0	17.4	2.4	191.4	92.5	277
7a	Se	—	X-ray	**au**	134.7	111.7	104.2	2.8	0.9	190.8	94.2	279
7b	Se	—	X-ray	**au**	135.1	111.1	104.5	3.9	2.1	190.6	93.3	277
12	S	—	X-ray	**f**	134.5	111.0	104.0	17.0	3.0	177.5	93.4	263
6	Te	Te	X-ray	**af**	134.9	115.2		1.7		211.4	89.3	297
5	Se	Se	X-ray	**af**	133.9	112.8		0.5		190.7	94.3	280

and 502 pm to vary, resulting in a non-centered Te atom. The degrees of overcrowding in the fjord regions of **14** as reflected in the intramolecular non-bonding distances between the fjord regions nitrogens and carbons/hydrogens, $H^8\cdots N^{8'}$, $H^1\cdots N^{1'}$, $C^8\cdots N^{8'}$ and $C^1\cdots N^{1'}$, are relatively small, 276 pm, 302 pm, 296 pm, and 288 pm, respectively. For comparison, the respective van der Waals contact distances are 321 pm ($C\cdots N$), 265 pm ($H\cdots N$).[37] Thus, the penetration in **14** is up to 12%. The $Te^{10}\cdots C^9$ non-bonding distance in **14** is 320 pm, while in **8**, the $Te\cdots C^9$ non-bonding distance is 315 pm, both considerably shorter than the van der Waals contact distance $Te\cdots C$ 379 pm.[37,38] The pyramidalization angles χ_9 and $\chi_{9'}$ in **14** are negligible. The stress of the overcrowding in **14** is solved by folding and a slight twisting. In **13**, the folding dihedral of the selenoxanthenylidene moiety is similar to **7b**, 62.6° *versus* 62.0°. The diazafluorenylidene moiety in **13** is almost planar. The penetration in the fjord regions of **13** and **12** are relatively small, up to 9% (**13**) and 10% (**12**), as reflected in the $C^1\cdots N^{1'}$ 295 ppm (**13**) and 290 pm (**12**). The most interesting feature in the molecular structures of the 1,8-diazafluorenylidene-chalcoxanthenes **12**–**14** is the high degrees of pyramidalization of C^9 (χ_9) 17.4° (**13**) and 17.0° (**12**), as compared with the small χ_9 values in **14**, **7**, and **8**, 2.2° (**14**), 2.8° (**7a**) and 8° (**8**). On the other hand, $\chi_{9'}$ is negligible. The high degree of pyramidalization in **13** points at an additional mode for solving the distress of overcrowding in the fjord regions when the fluorenylidene moiety is almost planar and the chalcoxanthenylidene moiety is highly folded. The high degrees of pyramidalization in **13** and **12** stem from the resistance of the diazafluorenylidene moieties in **12** and **13** to folding and from the limits in the degrees of folding of the selenoxanthylidene and thioxanthylidene moieties (due to the shorter $Se^{10}–C^{4a}$ /$Se^{10}–C^{10a}$ bonds and $S^{10}–C^{4a}$/$S^{10}–C^{10a}$ bonds as compared with the $Te^{10}–C^{4a}$/$Te^{10}–C^{10a}$ bonds in the telluroxanthylidene moiety of **14**). It should also be noted that this burden falls on C^9 in the chalcoxanthenylidene moieties and not on $C^{9'}$ of the diazafluorenylidene moieties. The crystal structure of **14** revealed short $Te^{10}\cdots C^3$ and $Te^{10}\cdots C^{8a}$ non-bonding distances 369.4 pm, and 364.3 pm, respectively (Fig. 3), shorter than the van der Waals $Te\cdots C$ contact distance 379 pm.[37,38] The crystal structures of **12** and **13** didn't indicate analogous short intermolecular non-bonding distances. In contrast to the crystal structures of **6** no short intermolecular $Te\cdots Te$ distances between the tellurium atom of one molecule and tellurium atom of neighboring molecules were found in the crystal structure of **14**.

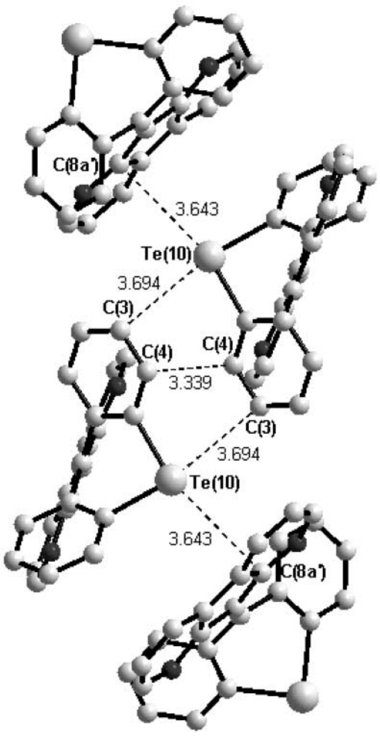

Fig. 3 Short Te–C intermolecular distances in the crystal structure of **14**.

NMR Spectroscopy

^1H-, ^{13}C-, ^{77}Se-, and ^{125}Te-NMR spectroscopic studies of the 1′,8′-diazafluorenylidene-chalcoxanthenes were carried out. Table 2 gives the ^1H-NMR chemical shifts of 1′,8′-diazafluorenylidene-chalcoxanthenes (**11**) *versus* fluorenylidene-chalcoxanthenes (**10**) and related homomerous bistricyclic enes. Table 3 gives the ^{13}C-NMR chemical shifts of **11** *versus* **10** and related homomerous bistricyclic enes. Table 4 gives the ^{77}Se- and ^{125}Te-NMR chemical shifts of **14**, **13**, and related compounds. Complete assignments were made through 2-dimensional correlation spectroscopy [COSY, heteronuclear single quantum coherence (HSQC), heteronuclear multiple bond coherence (HMBC)]. It is possible to distinguish qualitatively among the twisted conformation, the *anti*-folded conformation and the

Table 2 ^{1}H NMR Chemical shifts (δ) of **2**, **3**, **5**–**10**, **12**–**17**[a]

1	Y	X	[b]	H^1, H^8 $H^{1'}$,$H^{8'}$	H^2, H^7 $H^{2'}$, $H^{7'}$	H^3, H^6 $H^{3'}$ $H^{6'}$	H^4, H^5 $H^{4'}$, $H^{5'}$
8	Te	—	**au**	7.733	7.344	7.198	8.004
				6.934	6.934	7.247	7.658
14	Te	—	**f**	7.832	7.293	7.162	7.947
					8.256	7.137	7.833
7	Se	—	**au**	7.778	7.330	7.257	7.823
				7.192	6.946	7.257	7.659
13	Se	—	**f**	7.980	7.303	7.238	7.761
					8.282	7.154	7.888
10 (Y = S)	S	—	**au**	7.829	7.332	7.332	7.703
				7.358	6.975	7.273	7.547
12	S	—	**f**	8.109	7.318	7.318	7.633
					8.302	7.161	7.890
9	O	—	**t**	8.134	7.124	7.360	7.366
				7.889	7.066	7.268	7.724
15	O	—	**t**	8.701	7.162	7.506	7.388
					8.447	7.189	8.054
2	—	—	**t**	8.386	7.211	7.332	7.709
16	—	—	**t**	9.001	7.212	7.342	7.587
					8.626	7.258	8.003
17[19]	—	—	**t**	8.43	7.31	8.77	
6	Te	Te	**af**	6.796	6.879	6.963	7.801
5	Se	Se	**af**	6.787	6.904	7.072	7.656
3	O	O	**af**	7.146	6.877	7.226	7.270

[a] In $CDCl_3$ (relative to $CHCl_3$ $\delta = 7.26$ ppm). [b] Conformation: **au**: unevenly *anti*-folded; **af**: *anti*-folded; **t**: twisted.

Table 3 ^{13}C NMR Chemical shifts (δ) of **2**, **3**, **5**–**10**, **12**–**17**[a]

1	Y	X	C^1, C^8 $C^{1'}$, $C^{8'}$	C^2, C^7 $C^{2'}$, $C^{7'}$	C^3, C^6 $C^{3'}$, $C^{6'}$	C^4, C^5 $C^{4'}$, $C^{5'}$	C^{4a}, C^{10a} $C^{4a'}$, $C^{10a'}$	C^{8a}, C^{9a} $C^{8a'}$, $C^{9a'}$	C^9 $C^{9'}$
8	Te	—	129.10	127.57	127.16	136.99	118.94	142.39	145.74
			125.65	126.36	128.26	119.31	140.90	137.96	131.37
14	Te	—	131.38	127.07	125.96	135.84	116.26	141.18	151.60
				147.94	122.26	126.68	131.34	156.50	127.95
7	Se	—	129.30	126.60	127.25	131.23	133.55	136.61	140.33
			125.59	126.22	128.25	119.33	140.94	137.99	131.55
13	Se	—	132.13	124.86	127.31	129.81	131.38	136.91	146.78
				147.80	122.31	126.68	131.17	156.40	127.90
10 (Y = S)	S	—	129.03	126.12	127.30	128.68	136.53	137.29	137.29
			125.54	126.07	128.32	119.34	140.98	138.07	131.65
12	S	—	132.20	124.20	127.68	127.00	134.75	135.17	144.09
				147.65	122.26	126.65	131.00	156.32	127.68
9	O	—	130.03	122.79	129.93	117.63	154.02	124.80	130.86
			124.27	125.85	127.44	119.43	140.28	139.34	130.99
15	O	—	133.74	122.45	132.16	117.07	153.11	123.02	142.59
				147.41	120.64	126.95	128.81	157.00	123.92
2	—	—	126.73	126.85	129.15	119.89	141.31	138.28	141.01
16	—	—	130.57	127.07	130.97	119.24	142.94	138.48	148.71
				148.11	122.41	127.28	131.65	156.99	136.01
17[19]	—	—	133.52	122.91	151.41		158.48	131.89	136.52
6	Te	Te	130.67	127.02	126.57	134.98	118.01	141.27	143.69
5	Se	Se	130.47	126.18	126.68	129.47	132.42	137.44	137.44
3	O	O	128.31	122.40	128.12	117.08	155.48	124.92	121.44

[a] In $CDCl_3$ (relative to $CDCl_3$ $\delta = 77.01$ ppm).

Table 4 ^{77}Se and ^{125}Te NMR chemical shifts of bistricyclic enes and related compounds

Se Compd	X	Y	δ^{77}Se[a] (ppm)	$\Delta\delta$ (ppm)[b]	Te Compd	X	Y	δ^{125}Te[c] (ppm)	$\Delta\,\delta$ (ppm)[d]	δTe/δSe
21			334.7	0.0	**22**			473.4	0.0	1.40
7	Se	—	398.2	63.5	**8**	Te	—	620.9	147.5	1.56
13	Se	—	381.0	46.3	**14**	Te	—	589.9	145.8	1.55
5	Se	Se	366.3	31.6	**6**	Te	Te	574.1	73.7	1.49

[a] In $CDCl_3$ (relative to Me_2Se in $CDCl_3$).[40] [b] Relative to selenoxanthone.[40] [c] In $CDCl_3$ (relative to Me_2Te in C_6D_6).[40] [d] Relative to telluroxanthone.

syn-folded conformation of homomerous BAEs **1** in solution, using ^{1}H-NMR chemical shifts of the fjord protons H^1, H^8, $H^{1'}$, $H^{8'}$.[15] In heteromerous BAEs the task is less straightforward but still manageable. In **12**–**14**, the fjord region protons H^1 and H^8 of the chalcoxanthenylidene moiety appear at 8.109, 7.980, and 7.832 ppm, respectively. These molecules adopt folded conformations not only in the solid state but also in solution, as indicated in the chemical shifts of their fjord protons and in their yellow color. In **15**, the bridge in the central six membered ring is oxygen and the color of this molecule is purple. BAE **16**, in which both central rings are five-membered, is red. The chemical shifts of the fjord protons H^1, H^8, of **15** and **16** appear at low field, 8.701, 9.001 ppm, respectively. We conclude that both **15** and **16** adopt twisted conformations. This conclusion was verified by the UV/VIS spectra of **15**. Its purple color was recognized by the longest wavelength absorption at 521 nm. For comparison, the respective absorptions of **9**, **2**, **12**, **13**, **14**, **16**, **17** and **18** appear at 533[17](**9**), 458[39] (**2**), 402 (**12**), 402 (**13**), 426 (**14**), 433[18] (**16**), 416[19] (**17**) and 425–435 nm (sh)[18] (**18**). The related HOMO–LUMO gaps in **9** and **15**, as compared with **2** and **17** are attributed to higher degrees of pure twist of C^9=$C^{9'}$ and the dipolar aromatic structures in the former ($\omega = 40°$(**9**),[17] 30.2°(**2**),[6] 30.1°(**17**)[19]).

Comparisons between ^{1}H- and ^{13}C-NMR chemical shifts of the 1′,8′-diazafluorenylidene-chalcoxanthenes (**11**) and fluorenylidene-chalcoxanthenes (**10**), are summarized in Fig. 4: **14** *vs.* **8**, **13** *vs.* **7**, **12** *vs.* **10** (Y = S), **15** *vs.* **9**, and **16** *vs.* **2**. These comparisons illustrate the effect of the fjord nitrogens at positions 1′ and 8′ in **12**–**17** on the chemical shifts of the chalcoxanthylene and fluorenylide moieties. In the *anti*-folded **12**–**14**, the fjord protons are shifted downfield by 0.1–0.3 ppm, while in the twisted **15** and **16** the respective shifts are 0.56–0.62 ppm. In the *anti*-folded **12**–**14**, the fjord protons of the chalcoxanthene moieties are above or below the pyridine rings of the fluorenylidene moieties. This alignment minimizes the effect of the nitrogens. However, in the twisted **15** and **16**, the fjord protons are bucking towards the fjord nitrogens. Consequently, the effect of the nitrogens is more pronounced.

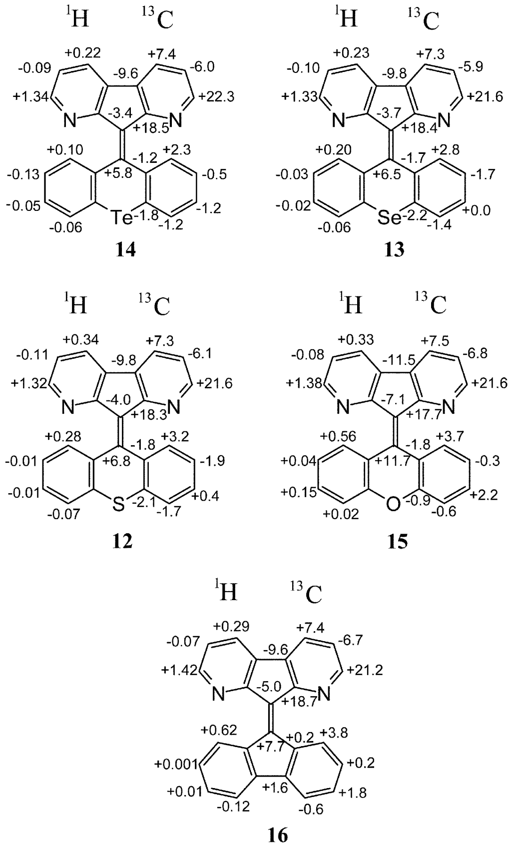

Fig. 4 Comparison between ^{1}H and ^{13}C-NMR chemical shifts of **11** and **10**.

Within the **11** series, upon going down in the chalcogen (column 16), from S to Te, the fjord protons are shifted upfield, in spite of the fact that the folding dihedrals of the diazafluorenylidene moieties are similar and are very small in **12**–**14**, 1.5–1.2°, indicating that the diazafluorenylidene moieties are almost planar. This effect is perhaps due to the differences in the distances $H^1 \cdots N^{1'}$, 258 pm (**12**), 279 pm (**13**), and 302 pm (**14**). The variance in the chemical shifts of H^1, H^8 (chalcoxanthenylidene moiety) in **12**–**14** is wider than that of H^1, H^8 (chalcoxanthenylidene moiety) in **10**: *e.g.*, δ(**12**) − δ(**14**) = 0.277 *versus* δ(**10**, Y = S) − δ(**7**) = 0.096.

The ^{13}C-NMR spectra of **2**, **3**, **5**–**10**, **12**–**16** (Table 3) indicate that chemical shifts of the fjord regions C^1 and C^8 of the chalcoxanthenylidene moieties of **12**–**16** are very similar: 132.20 (**12**), 132.13 (**13**), 131.38 (**14**), 133.74 (**15**), 130.57 (**16**). The fjord carbons are less sensitive to the overall conformations, folded or twisted, as compared with the fjord hydrogens. There is a certain shift to a low field in comparison to **10** and to **2**. A comparison of **10** and **11** indicates that chemical shifts of C^1 and C^8 do shift to low field: the range of the shift is 2.3–3.8 ppm. The shifts are somewhat larger in the twisted **15** and **16** as compared to the folded **12**–**14**.

The most interesting observation derived from the comparison of the NMR chemical shifts of the diazafluorenylidene series **11** with the fluorenylidene series **10** is the trend in the chemical shifts of C^9 and $C^{9'}$ (Table 3 and Fig. 4) $\Delta\delta$ ($C^{9'}$) = δ(**11**) − δ(**10**) are negative (upfield) −3.4 (**14**), −3.7 (**13**), −4.0 (**12**), −7.1 (**15**), −5.0 ppm (**16**) while $\Delta\delta$ (C^9) = δ(**11**) − δ(**10**) are positive (downfield) +5.8 (**14**), +6.5 (**13**), +6.8 (**12**), +11.7 (**15**), +7.7 ppm (**16**). These differences are more pronounced in the twisted BAEs than in the *anti*-folded BAEs. The twisted oxygen-bridged pair **15/9** shows the highest values of $\Delta\delta$. Moreover in **9**, δ (C^9) − δ($C^{9'}$) = −0.13 ppm, while in **15**, δ (C^9) − δ ($C^{9'}$) = +18.7 ppm. In the *anti*-folded BAEs there is a slight decrease in $\Delta\delta$ (C^9) and $\Delta\delta$ ($C^{9'}$) in the series S(**12**) > Se (**13**) > Te (**14**). In order to obtain a deeper comprehension of the significance of the differences in the chemical shifts in the twisted pairs **15/9** and **16/2**, it is helpful to consider the respective differences in the precursors 9-diazo-9*H*-1,8-diazafluorene (**28**) and 9*H*-1,8-diazafluoren-9-one (**19**) *versus* 9-diazo-9*H*-fluorene (**31**) and 9*H*-fluoren-9-one (**32**), respectively. (Fig. 5). These systems were selected for comparison because of the opposite character of their substituents: the carbonyl oxygen of **19** and **32** is an acceptor while the diazo groups of **28** and **31** are

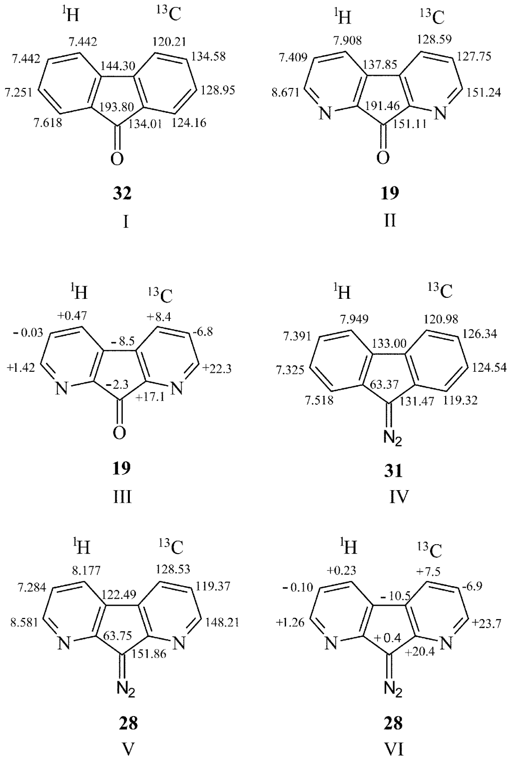

Fig. 5 Comparison of ^{1}H and ^{13}C-NMR chemical shifts: **32** *versus* **19** and **31** *versus* **28**.

Table 5 Crystallographic data for **12**–**14**

	Compound		
	12	**13**	**14**
Space group	*Pmn*2$_1$	*Pmn*2$_1$	*P*2$_1$/*n*
Crystal system	Orthorhombic	Orthorhombic	Monoclinic
a/pm	1881.1(4)	1871.3(3)	1257.9(2)
b/pm	970.2(3)	955.3(2)	1192.0(2)
c/pm	463.9(1)	483.1(1)	1220.2(2)
α/deg	90.0	90.0	90.0
β/deg	90.0	90.0	92.68(1)
γ/deg	90.0	90.0	90.0
V/pm^3	846.6 × 10^6	863.6 × 10^6	1827.6 × 10^6(6)
Z	2	2	4
ρ_{calc}/g cm^{-3}	1.42	1.57	1.66
$\mu(\mathrm{K}_\alpha)$/cm^{-1}	17.67	21.59	16.38
Diffractometer	ENRAF-NONIUS CAD4	Philips PW1100/20	Philips PW1100/20
Radiation λ/pm	154.178	71.069	71.069
$2\theta_{\mathrm{max}}$/deg	140	55	60
No. of unique reflections	998	1206	5561
No. of reflections with $I > 3\sigma_I$	880	1002	3444
R	0.038	0.036	0.047
R_w	0.050	0.042	0.065

donors. In these pairs the carbons that are in close proximity to the fjord nitrogens, C^2, C^7, C^{8a} and C^{9a}, are shifted downfield: $\Delta\delta$ (C^2, C^7) = 22.3 (**19/32**) and 23.7 ppm (**28/31**) $\Delta\delta$ (C^{8a}, C^{9a}) = 17.1 (**19/32**) and 20.4 ppm (**28/31**); This effect is maintained in all the pairs under study (Fig. 4): **14/8**, **13/7**, **12/10** (X = S), **15/9**, and **16/2**. Thus, the chemical shifts of the neighboring C^2, C^7, C^{8a}, and C^{9a}, in the 1,8-diazafluorene moiety are primarily determined by N^1 and N^8. An analogous picture emerges in the chemical shifts $\Delta\delta$ (C$^{1'}$) of the other aromatic carbons of the fluoreylidene/1,8-diazafluorenylidene moieties. They are hardly sensitive to the bridge of the opposing tricyclic moiety. The special character of twisted **15** is manifold in the remarkably high value of $\Delta\delta\delta$ (**15/9**) = [δ(C^9)(**15**) − δ(C$^{9'}$)(**15**)] − [δ(C^9)(**9**) − δ(C$^{9'}$)(**9**)] = 18.8 ppm, as compared with the respective $\Delta\delta\delta$ value of **14/8** (9.3 ppm), **13/7** (10.1 ppm), **12/10** (10.8 ppm), and **16/2** (12.7 ppm). This effect may be interpreted in terms of significant contributions of zwitterion structures. It is doubtful, however, whether the contributions of the aromatic xanthylium-diazafluorenide structure (**15a**) is more pronounced in **15** than that of the xanthylium-fluorenide structure (**9a**) in **9**.

The ^{77}Se and ^{125}Te NMR chemical shifts of **13** and **14** (Table 4) were very helpful, due to their sensitivity, in monitoring the progress of the syntheses leading to these selenium- and tellurium-bridged heteromerous bistricyclic enes. The chemical shifts of the chalcogen atoms in the **13** and **14** are shifted upfield, relative to **7** and **8**, δ^{77}Se (**13**) − δ^{77}Se (**7**) = −17.2 ppm and δ^{125}Te (**14**) – δ^{125}Te (**8**) = 31.0 ppm, although the δ^{125}Te/δ^{77}Se ratio between the heteromerous bistricyclic enes pairs **14/13** and **8/7** is almost the same, 1.55 and 1.56, respectively. Thus, the presence of the nitrogens at positions 1′,8′ in **13** and **14** causes shielding of the selenium and the tellurium, relative to **7** and **8**, in spite the fact that the diazafluorenylidene moieties are almost planar.

Conclusion

In conclusion, the introduction of nitrogen atoms in the fjord regions of **12**–**16** generates a new heterocyclic series of bistricyclic aromatic enes based on the 1,8-diazafluorenylidene functionality. This variation of the theme affects the modes of deviations from planarity due to overcrowding. The potential push–pull character of 1′,8′-diazafluorenylidene-chalcoxanthenes **12**–**15** is possibly indicated in twisted **15**, but not in folded **12**–**14**. On the other hand, 1,8-diazafluoren-9-one (**19**), the important latent fingerprint agent and the starting material in the syntheses of **12**–**16**, is not a push–pull, but a "pull–pull" system. Its diazafluorenylidene and carbonyl functionalities are polarized in the same direction.

Experimental

Melting points are uncorrected. All NMR spectra were recorded with a Bruker DRX 400 spectrometer; ^{1}H NMR spectra were recorded at 400.1 MHz using CDCl$_3$ as solvent and as internal standard (δ(CHCl$_3$) = 7.26 ppm). ^{13}C NMR spectra were recorded at 100.6 MHz using CDCl$_3$ as solvent and as internal standard (δ(CDCl$_3$) = 77.01 ppm). ^{77}Se NMR spectra were recorded at 76.3 MHz using CDCl$_3$ as a solvent and selenoxanthone (**21**) as external standard δ = 334.7 ppm (relative to Me$_2$Se in CDCl$_3$).[40] ^{125}Te NMR spectra were recorded at 126.2 MHz using CDCl$_3$ as solvent and telluroxanthone (**22**) as external standard δ = 473.6 ppm (relative to Me$_2$Te in C$_6$D$_6$, in DMSO-d$_6$, δ(**22**) = 471.5 ppm).[40] UV/VIS spectra were measured using an UVIKON 860 spectrometer. IR spectra were measured with a Perkin Elmer System 2000 FT-IR spectrometer.

Elemental microanalyses were determined by Chemisar Laboratories Inc., N. Guelph, Ontario Canada. Single crystals were obtained by slow sublimation in a high vacuum sealed tube at 200–250 °C in a Büchi GKR 50 oven.

X-Ray crystallographic analysis: the crystal data of **12**–**14** are given in Table 5.† The lattice parameters were obtained by a least-squares fit of 24 centered reflections. Intensity data were collected using the ω–2θ technique. The scan width, $\Delta\omega$, for each reflection was 1.00 + 0.35tanθ for Mo radiation and 0.80 + 0.15tanθ for Cu radiation. The intensities of three standard reflections were monitored during data collection, and no decay was observed. Intensities were corrected for Lorentz and polarization effects. The positions of all non-hydrogen atoms were obtained using the results of the SHELXS-86 direct method analysis.[41] After several cycles of refinements the positions of the hydrogen atoms were either found, for compound **14**, or calculated, for **12** and **13**, and added to the refinement process. All non-hydrogen atoms were refined anisotropically, while the positions of hydrogen atoms were refined isotropically for **14** or kept fixed, using a riding model for compounds **12** and **13**. The refinement proceeded to convergence by minimizing the function $\Sigma w(|F_o| - |F_c|)^2$ with $w = \sigma_F^{-2}$.

9*H*-1,8-Diazafluoren-9-one (19)

Ketone **19**, purchased from Fluka, is a yellow powder, mp 229–231 °C (lit.[35,36] mp 205 °C, 209 °C). ^{1}H NMR (CDCl$_3$): δ 7.409

---

† CCDC reference numbers 207024–207026. See http://www.rsc.org/suppdata/ob/b3/b303041e/ for crystallographic data in .cif or other electronic format.

(td, $^3J = 7.7$ Hz,$^3J = 4.9$ Hz, 2H, H^3, H^6), 7.908 (dd, $^3J = 7.7$ Hz, $^4J = 1.5$ Hz, 2H, H^4, H^5), 8.671 (dd, $^3J = 4.9$ Hz, $^4J = 1.4$ Hz, 2H, H^2, H^7). ^{13}C NMR (CDCl$_3$): δ 127.75 (C^3, C^6), 128.59 (C^4, C^5), 137.85 (C^{4a}, C^{4b}), 151.11 (C^{8a}, C^{9a}), 151.24 (C^2, C^7), 191.46 (C^9).

9*H*-1,8-Diazafluoren-9-one hydrazone (29)

Hydrazone **29** was prepared from **19** according to the literature, yield 78%; dec 186–188 °C (lit.[18] dec 176 °C). ^{1}H NMR (CDCl$_3$): δ 7.237 (td, $^3J = 7.7$ Hz, $^3J = 5.0$ Hz, 1H, H^6), 7.304 (td, $^3J = 7.7$ Hz, $^3J = 5.0$ Hz, 1H, H^3), 7.972 (dd, $^3J = 7.7$ Hz, $^4J = 1.5$ Hz, 1H, H^5), 8.061 (dd, $^3J = 7.7$ Hz, $^4J = 1.5$ Hz, 1H, H^4), 8.564 (dd, $^3J = 5.0$ Hz, $^4J = 1.5$ Hz, 1H, H^7), 8.602 (dd, $^3J = 5.0$ Hz, $^4J = 1.5$ Hz, 1H, H^2). ^{13}C NMR (CDCl$_3$): δ 121.39 (C–H), 121.92 (C-H), 127.75 (C-H), 127.76 (C-H), 128.51 (C), 129.94 (C), 134.57 (C), 147.53 (C-H), 149.46 (C-H), 151.34 (C), 154.68 (C). IR, Nujol ν_{max}/cm^{-1}: 3300 (N–H).

9-Diazo-9*H*-1,8-diazafluorene (28)

(a) Diazo **28** was prepared from **29** according to the literature,[18] with certain modifications. Dried hydrazone **29** (0.199 g, 1.02 mmol), mercuric oxide (0.453 g, 2.09 mmol) and anhydrous sodium sulfate (0.261 g, 1.83 mmol) were ground together for a few minutes then transferred to a dry flask equipped with a magnetic stirrer protected by a CaCl$_2$ tube and containing dry Et$_2$O (20 mL). After 1 h, a freshly prepared, concentrated solution of KOH in ethanol was added (10 drops). The color of the solution changed gradually from yellow to grey–black. The reaction was stirred at rt for 4 h. The progress of the reaction was monitored by TLC on silica gel (toluene–chloroform–Et$_3$N 9 : 1 : 1 $R_f = 0.63$). The solution was filtered off and the residue was washed with Et$_2$O. The combined organic fractions were evaporated under reduced pressure, to give **28** as orange crystals 0.143 g, yield 73%; mp 92–96 °C (lit.[18] mp 94–95 °C).

(b) A stirred solution of hydrazone **29** (0.300 g, 1.53 mmol) in anhydrous Et$_2$O (50 mL) protected by a CaCl$_2$ tube, was cooled to 0 °C, whereupon MgSO$_4$ (0.350 g), Ag$_2$O (0.530 g, 2.29 mmol) and a saturated solution of KOH in methanol (1 mL) were added. The reaction mixture was stirred for 4 h at *ca.* 0 °C and the temperature raised to rt and stirred for 20 h. The color changed gradually from yellow to orange. The reaction was monitored with TLC (toluene–chloroform–Et$_3$N 9 : 1 : 1 $R_f = 0.63$). Workup as in procedure (a) gave orange crystals of **28** (0.214 g), yield 72%; mp 92–96 °C (lit.[18] mp 94–95 °C). ^{1}H NMR (CDCl$_3$): δ 7.284 (td $^3J = 7.8$ Hz, $^3J = 4.9$ Hz, 2H, H^3, H^6), 8.177 (td, $^3J = 7.7$ Hz, $^3J = 1.6$ Hz, 2H, H^4, H^5), 8.581 (dd, $^3J = 4.9$ Hz, $^4J = 1.4$ Hz, 2H, H^4, H^5). ^{13}C NMR (CDCl$_3$): δ 63.75 (C^9), 119.37 (C^3, C^6), 122.49 (C^{4a}, C^{4b}), 128.53 (C^4, C^5), 148.21 (C^2, C^7), 151.86 (C^{8a}, C^{9a}). IR, KBr λ_{max}/cm^{-1}: 2083 (N≡N).

9-(9′*H*-1,8-Diazafluoren-9′-ylidene)-9*H*-thioxanthene (12)

To a stirred solution of diazo **28** (0.087 g, 0.448 mmol) in anhydrous benzene (30 mL) and protected by a CaCl$_2$ tube, thione **24** (0.102 g, 0448 mmol) was added. The reaction mixture was refluxed for 80 h. The termination of the reaction was determined by NMR. The color of the reaction mixture was dark. The mixture was cooled to rt, and the solvent was removed under reduced pressure. Trituration of the crude product in hot ethanol gave a precipitate, which was filtered off. A greenish yellow powder was obtained 0.124 g, yield 77%; mp 261–263 °C. A sample of **12** for analysis was purified by column chromatography on silica gel using CH$_2$Cl$_2$ as eluent. ^{1}H NMR (CDCl$_3$): δ 7.161 (t, $^3J = 7.7$ Hz, $^3J = 4.9$ Hz, 2H, H$^{3'}$, H$^{6'}$), 7.318 (m, 4H, H^2, H^7, H^3, H^6), 7.633 (m, 2H, H^4, H^5), 7.890 (dd, $^3J = 7.6$ Hz, $^3J = 1.6$ Hz, 2H, H$^{4'}$,H$^{5'}$), 8.109 (m, 2H, H^1, H^8), 8.302 (dd, $^3J = 4.8$ Hz, $^4J = 1.7$ Hz, 2H, H$^{2'}$, H$^{7'}$). ^{13}C NMR (CDCl$_3$): δ 122.26 (C$^{3'}$, C$^{6'}$), 124.20 (C^2, C^7), 126.65 (C$^{4'}$, C$^{5'}$), 127.00 (C^4, C^5), 127.46 (C^3, C^6), 127.68 (C$^{9'}$), 131.00 (C$^{4a'}$, C$^{4b'}$), 132.20 (C^1, C^8), 134.75 (C^{4a}, C^{10a}), 135.17 (C^{9a}, C^{8a}), 144.09 (C^9), 147.65 (C$^{2'}$, C$^{7'}$), 156.32 (C$^{8a'}$, C$^{9a'}$). UV/VIS (cyclohexane): $c = 9.392 \times 10^{-5}$ M. λ_{max}/nm (ε): 339 (13,032), 402 (12819). Calc. for C$_{24}$H$_{14}$N$_2$S: C, 79.53; H, 3.89; N, 7.72; S, 8.84. Found: C, 79.17; H, 3.96; N, 7.60; S, 8.78%.

9-(9′*H*-1,8-Diazafluoren-9′-ylidene)-9*H*-selenoxanthene (13)

To a stirred solution of diazo **28** (0.090 g, 0.464 mmol) in anhydrous benzene (30 mL) and protected by a CaCl$_2$ tube, thione **25** (0.127 g, 0464 mmol) was added. The reaction mixture was refluxed for 52 h. The termination of the reaction was determined by NMR. The color of the reaction mixture was dark. The mixture was cooled to rt, and the solvent was removed under reduced pressure Trituration of the crude product in hot ethanol gave a precipitate, which was filtered off. A greenish yellow powder of **13** was obtained 0.136 g, yield 72%; mp 279–281 °C. A sample of **13** for analysis was purified by column chromatography on silica gel using CH$_2$Cl$_2$ as eluent. ^{1}H NMR (CDCl$_3$): δ 7.154 (t, $^3J = 7.7$ Hz, $^3J = 4.9$ Hz, 2H, H$^{3'}$, H$^{6'}$), 7.238 (td, $^3J = 7.5$ Hz, $^4J = 1.4$ Hz, 2H, H^3, H^6), 7.303 (td, $^3J = 7.4$ Hz, $^4J = 1.4$ Hz, 2H, H^2, H^7), 7.761 (ddd, $^3J = 7.6$ Hz, $^4J = 1.3$ Hz, $^5J = 0.5$ Hz, 2H, H^4, H^5), 7.888 (dd, $^3J = 7.7$ Hz, $^4J = 1.7$ Hz, 2H, H$^{4'}$,H$^{5'}$), 7.980 (ddd, $^3J = 7.6$ Hz, $^4J = 1.7$ Hz, 2H, H^1, H^8), 8.282 (dd, $^3J = 4.8$ Hz, $^4J = 1.7$ Hz, 2H, H$^{2'}$, H$^{7'}$). ^{13}C NMR (CDCl$_3$): δ 122.31 (C$^{3'}$, C$^{6'}$), 124.86 (C^2, C^7), 126.68 (C$^{4'}$, C$^{5'}$), 127.31 (C^3, C^6), 127.90 (C$^{9'}$), 129.81 (C^4,C^5), 131.17 (C$^{4a'}$, C$^{4b'}$), 131.38 (C^{4a}, C^{10a}), 132.13 (C^1, C^8), 136.91 (C^{8a}, C^{9a}), 146.78 (C^9), 147.80 (C$^{2'}$, C$^{7'}$), 156.40 (C$^{8a'}$, C$^{9a'}$).

^{77}Se NMR (CDCl$_3$): δ 381.03. UV/VIS (cyclohexane): $c = 4.352 \times 10^{-5}$ M. λ_{max}/nm (ε): 333 (11098), 402 (6570). Calc. for C$_{24}$H$_{14}$N$_2$Se: C, 76.66; H, 3.93; N, 6.84; Se, 19.38. Found: C, 76.63; H, 3.94; N, 6.72; Se, 19.05%.

9-(9′*H*-1,8-Diazafluoren-9′-ylidene)-9*H*-telluroxanthene (14)

To a stirred solution of thione **26** [freshly prepared from ketone **22** (0.200 g, 0.649 mmol) and Lawesson's reagent (0.134 g, 0.325 mmol), in dried benzene (30 mL)] in anhydrous benzene (30 mL) protected by a CaCl$_2$ tube, diazo derivative **28** (0.125 g, 0.664 mmol) was added. The reaction mixture was refluxed for 48 h. The color of the reaction mixture was dark. The mixture was cooled to rt, and the solvent was removed under reduced pressure. Trituration of the crude product in hot ethanol gave a precipitate, which was filtered off. A greenish yellow powder was obtained, 0.154 g. NMR showed that a mixture of **14** and the corresponding thiiran was obtained. The latter was not isolated. This mixture, protected by a CaCl$_2$ tube, was treated with PPh$_3$ (0.081 g, 0.310 mmol) in anhydrous benzene (30 mL) and refluxed for 8 h. The solvent was removed under reduced pressure. Trituration of the crude product in hot ethanol gave a precipitate, which was filtered off. A yellow powder of **14** was obtained 0.130 g; mp 299–300 °C. A sample of **14** for analysis was purified by column chromatography on silica gel using CH$_2$Cl$_2$ as eluent. Trituration ^{1}H NMR (CDCl$_3$): δ 7.137 (t, $^3J = 7.6$ Hz, $^3J = 4.8$ Hz, 2H, H$^{3'}$, H$^{6'}$), 7.162 (td, $^3J = 7.5$ Hz, $^4J = 1.4$ Hz, 2H, H^3, H^6), 7.293 (td, $^3J = 7.5$ Hz, $^4J = 1.2$ Hz, 2H, H^2, H^7), 7.832 (ddd, $^3J = 7.7$ Hz, $^4J = 1.4$ Hz, $^5J = 0.4$ Hz, 2H, H^1, H^8), 7.883 (dd, $^3J = 7.7$ Hz, $^3J = 1.7$ Hz, 2H, H$^{4'}$, H$^{5'}$), 7.947 (ddd, $^3J = 7.6$ Hz, $^4J = 1.4$ Hz, $^5J = 0.4$ Hz, 2H, H^4, H^5), 8.256 (dd, $^3J = 4.8$ Hz, $^4J = 1.7$ Hz, 2H, H$^{2'}$, H$^{7'}$). ^{13}C NMR (CDCl$_3$): δ 116.26 (C^{4a}, C^{10a}), 122.26 (C$^{3'}$, C$^{6'}$), 125.96 (C^2, C^7), 126.68 (C$^{4'}$, C$^{5'}$), 127.07 (C^3, C^6), 127.95 (C$^{9'}$), 131.34 (C$^{4a'}$, C$^{4b'}$), 131.38 (C^1, C^8), 135.84 (C^4, C^5), 141.18 (C^{8a}, C^{9a}), 147.94 (C$^{2'}$, C$^{7'}$), 151.60 (C^9), 156.50 (C$^{8a'}$, C$^{9a'}$). ^{125}Te NMR (CDCl$_3$): δ 589.95. UV/VIS (cyclohexane): $c = 1.15 \times 10^{-4}$ M. λ_{max}/nm (ε): 333 (12991), 426 (2125). Calc. for C$_{24}$H$_{14}$N$_2$Te: C, 62.94; H, 3.08; N, 6.11; Te, 27.90. Found: C, 62.89; H, 2.87; N, 6.07; Te, 27.49%.

9-(9′*H*-1,8-Diazafluoren-9′-ylidene)-9*H*-xanthene (15)

To a stirred solution of diazo **28** (0.050 g, 0.255 mmol) in anhydrous benzene (10 mL) and protected by a CaCl$_2$ tube, thione **27** (0.051 g, 0.243 mmol) was added. The reaction mixture was refluxed for 125 h. The termination of the reaction was determined by NMR. The solution was evaporated under reduced pressure. Crude **15** dissolved in CH_2Cl_2 was introduced on top of the chromatography column. The color of the fractions on the column containing **15** were blue. NMR showed that **15** partially decomposed to **23** on the silica gel. Further purification was performed by sublimation at 170 °C/0.05 torr. Purple crystals of **15**, with gold sparkling were obtained by the sublimation. ^{1}H NMR ($CDCl_3$): δ 7.162 (td, $^3J = 8.3$ Hz, $^3J = 6.9$ Hz, $^4J = 1.3$ Hz, 2H, H^2, H^7), 7.189 (t, $^3J = 7.6$ Hz, $^3J = 4.8$ Hz, 2H, H$^{3'}$, H$^{6'}$), 7.388 (ddd, $^3J = 8.3$ Hz, $^4J = 1.3$ Hz, $^5J = 0.4$ Hz, 2H, H^4, H^5), 7.506 (td, $^3J = 8.4$ Hz, $^3J = 7.0$ Hz, $^4J = 1.5$ Hz, 2H, H^3, H^6), 8.054 (dd, $^3J = 7.7$ Hz, $^4J = 1.7$ Hz, 2H, H$^{4'}$, H$^{5'}$), 8.447 (dd, $^3J = 4.8$ Hz, $^4J = 1.7$ Hz, 2H, H$^{2'}$, H$^{7'}$), 8.701 (ddd, $^3J = 8.3$ Hz, $^4J = 1.6$ Hz, $^5J = 0.4$ Hz, 2H, H^1, H^8). ^{13}C NMR ($CDCl_3$): δ 117.07 (C^4, C^5), 120.64 (C$^{3'}$, C$^{6'}$), 122.45 (C^2, C^7), 123.02 (C^{8a}, C^{9a}), 123.92 (C$^{9'}$), 126.95 (C$^{4'}$, C$^{5'}$), 128.81 (C$^{4a'}$, C$^{4b'}$), 132.16 (C^3, C^6), 133.74 (C^1, C^8), 142.59 (C^9), 147.41 (C$^{2'}$, C$^{7'}$), 153.11 (C^{4a}, C^{10a}), 157.00 (C$^{8a'}$, C$^{9a'}$). UV/VIS (cyclohexane qualitative): λ_{max}/nm: 521, 386, 354. MS, *m*/*z* (% molecular ion): 347.11027 (6.13%, $^{12}C_{22}{}^{13}C_2H_{13}N_2O$), no molecular ion (0% $^{12}C_{24}H_{14}N_2O$), 346.10674 (35.18%, $^{12}C_{23}{}^{13}C_1H_{13}N_2O$), 345.10363 (100%, $^{12}C_{24}H_{13}N_2O$), 173.55619 (1.74%, $^{12}C_{22}{}^{13}C_2H_{13}N_2O/2$,), 173.05420 (6.87%, $^{12}C_{23}{}^{13}C_1H_{13}N_2O/2$), 172.54895 (4.86%. $^{12}C_{24}H_{13}N_2O$), 172.04688 (16.04%, $^{12}C_{24}H_{12}N_2O/2$).

9-(9′*H*-1,8-Diazafluoren-9′-ylidene)-9*H*-fluorene (16)

To a stirred solution of diazo **28** (0.100 g, 0.555 mmol) in anhydrous benzene (30 mL) and protected by a $CaCl_2$ tube, thione **30** (0.114 g, 0.580 mmol) was added. The reaction mixture was refluxed for 1 h and then kept at 70 °C (oil bath) for 72 h. The termination of the reaction was determined by NMR. The mixture was cooled to rt, and the solvent was removed under reduced pressure Trituration of the crude product in hot ethanol gave a precipitate, which was filtered off. Red **16** was obtained. Mp 245–247 °C (dec) (lit.[18] 243 °C). ^{1}H NMR ($CDCl_3$): δ 7.212 (td, $^3J = 7.9$ Hz, $^3J = 7.5$ Hz, $^4J = 1.2$ Hz, 2H, H^2, H^7), 7.258 (td, $^3J = 7.7$ Hz, $^3J = 5.0$ Hz, 2H, H$^{3'}$, H$^{6'}$), 7.342 (td, $^3J = 7.4$ Hz, $^4J = 1.0$ Hz, 2H, H^3, H^6), 7.587 (ddd, $^3J = 7.5$ Hz, $^4J = 1.2$ Hz, $^5J = 0.7$ Hz, 2H, H^4, H^5), 8.003 (dd, $^3J = 7.7$ Hz, $^4J = 1.4$ Hz, 2H, H$^{4'}$,H$^{5'}$), 8.626 (dd, $^3J = 4.8$ Hz, $^4J = 1.6$ Hz, 2H, H$^{2'}$, H$^{7'}$), 9.001 (dd, $^3J = 7.9$ Hz, $^4J = 1.0$ Hz, $^5J = 0.7$ Hz, 2H, H^1, H^8). ^{13}C NMR ($CDCl_3$): δ 119.24 (H^4, H^5), 122.41 (C$^{3'}$, C$^{6'}$), 127.07 (C^2, C^7), 127.28 (C$^{4'}$, C$^{5'}$), 130.57 (C^1, C^8), 130.97 (C^3, C^6), 131.65 (C$^{4a'}$, C$^{4b'}$), 136.01 (C$^{9'}$), 138.48 (C^{8a}, C^{9a}), 142.94 (C^{4a}, C^{4b}), 148.11 (C$^{2'}$, C$^{7'}$), 148.71 (C^9), 156.99 (C$^{8a'}$, C$^{9a'}$).

Acknowledgements

The authors thank Mr. P. Ulrich Biedermann for fruitful discussions and helpful comments.

References

1 G. Shoham, S. Cohen, R. M. Suissa and I. Agranat, in: *Molecular Structure Chemical Reactivity and Biological Activity*, eds. J. J. Stezowski, J.-L. Huang and M.-C. Shao, Oxford University Press, Oxford, 1988, p. 290.
2 J. Sandström, in: *The Chemistry of Double-Bonded Functional Groups*, Supplement A3, ed. S. Patai, Wiley, New York, 1997, p. 1253.
3 P. U. Biedermann, J. J. Stezowski and I. Agranat, in: *Advances in Theoretically Interesting Molecules*, Vol. 4, ed., R. P. Thummel, JAI Press, Stamford, CN, 1998, p. 245.
4 P. U. Biedermann, J. J. Stezowski and I. Agranat, *Eur. J. Org. Chem.*, 2001, 15.
5 P. U. Biedermann, J. J. Stezowski and I. Agranat, *Chem. Commun.*, 2001, 954.
6 P. U. Biedermann, A. Levy, J. J. Stezowski and I. Agranat, *Chirality*, 1995, **7**, 199.
7 W. Luef and R. Keese, *Top. Stereochem.*, 1991, **20**, 231.
8 Y. Tapuhi, M. R. Suissa, S. Cohen, P. U. Biedermann, A. Levy and I. Agranat, *J. Chem. Soc., Perkin Trans. 2*, 2000, 93.
9 B. L. Feringa, W. F. Jager and B. de Lange, *Tetrahedron Lett.*, 1992, **33**, 2887.
10 N. A. Bailey and S. E. Hull, *Acta Crystallogr., Sect. B*, 1978, **34**, 3289.
11 J.- S. Lee and S. C. Nyburg, *Acta Crystallogr., Sect. C*, 1985, **41**, 560.
12 J. F. D. Mills and S. C. Nyburg, *J. Chem. Soc.*, 1963, 308.
13 E. Harnik and G. M. J. Schmidt, *J. Chem. Soc.*, 1954, 3295.
14 K. S. Dichmann, S. C. Nyburg, F. H. Pickard and J. A. Potworowski, *Acta Crystallogr., Sect. B*, 1974, **30**, 27.
15 A. Levy, P. U. Biedermann, S. Cohen and I. Agranat, *J. Chem. Soc., Perkin Trans. 2*, 2000, 725.
16 A. Levy, P. U. Biedermann, S. Cohen and I. Agranat, *J. Chem. Soc., Perkin Trans. 2*, 2001, 2329.
17 A. Levy, P. U. Biedermann and I. Agranat, *Org. Lett.*, 2000, **2**, 1811.
18 A. Schönberg and K. Junghans, *Chem. Ber.*, 1962, **94**, 2137.
19 M. Riklin, A. von Zelewsky, A. Bashall, M. McPartlin, A. Baysal, J. A. Connor and J. D. Wallis, *Helv. Chim. Acta*, 1999, **82**, 1666.
20 M. Querol, H. Stoekli-Evans and P. Belser, *Org. Lett.*, 2002, **4**, 1067.
21 C. A. Pounds, R. Grigg and T. Mongkolaussavaratana, *J. Forensic Sci.*, 1990, **35**, 169–175.
22 R. Grigg, T. Mongkolaussavaratana, C. A. Pounds and S. Sivagnanam, *Tetrahedron Lett.*, 1990, **31**, 7215–7218.
23 R. E. Grigg, C. A. Pounds, T. Mongkolaussavaratana, “Fingerprint Reagent”, U. S. Patent 5,221,627, 22.06.1993 (Priority date 09.11.1988 GB 8,826,237); EP Patent 442959 B1, 31.08.1994.
24 J. Almog, “Fingerprints Development by Ninhydrin and Its Analogues”, in *Advances in Forensic Technology*, 2nd Edition, H. C. Lee and R. E. Gaensslen, Eds., CRC Press, Boca Raton, FL, 2001, pp. 177–209.
25 D. H. R. Barton, Ed., *Reason and Imagination: Reflections on Research in Organic Chemistry: Selected Papers of Derek H. R. Barton*, Imperial College Press and World Scientific, Singapore, 1996, Vol. 6, pp. 489.
26 D. H. R. Barton and B. J. Wills, *J. Chem. Soc., Perkin Trans. 1*, 1972, 305.
27 D. H. R. Barton, F. S. Guziec and I. Shahak, *J. Chem. Soc., Perkin Trans. 1*, 1974, 1794.
28 R. Lesser and R. Weiß, *Ber. Dtsch. Chem. Ges.*, 1914, **47**, 2510.
29 K. Šindelàr, E. Svàtek, J. Metyšovà, J. Metys and M. Protiva, *Collect. Czech. Chem. Commun.*, 1969, **34**, 3792.
30 I. D. Sadekov and V. I. Minkin, *Adv. Heterocycl. Chem.*, 1995, **63**, 1.
31 I. D. Sadekov, A. A. Ladatko and V. I. Minkin, *Khim. Geterotsikl. Soedin.*, 1980, 1342.
32 S. Scheibye, R. Shabana and S.-O. Lawesson, *Tetrahedron*, 1982, **38**, 993.
33 M. P. Cava and M. I. Levinson, *Tetrahedron*, 1985, **41**, 5061.
34 B. S. Pedersen, S. Scheibye, N. H. Nilsson and S.-O. Lawesson, *Bull. Soc. Chim. Belg.*, 1978, **87**, 223.
35 J. Druey and P. Schmidt, *Helv. Chim. Acta*, 1950, **33**, 1080.
36 K. Kloc, J. Mlochowski and Z. Szulc, *J. Prakt. Chem.*, 1977, **319**, 959.
37 Y. V. Zefirov, *Crystallog. Rep.*, 1997, **42**, 111.
38 A. Bondi, *J. Phys. Chem.*, 1964, **68**, 441.
39 E. D. Bergamann, *Prog. Org. Chem.*, 1955, **3**, 81.
40 W. Nakanishi, Y. Yamamoto, S. Hayashi, H. Tukada and H. Iwamura, *J. Phys. Org. Chem.*, 1990, **3**, 369.
41 G. M. Sheldrick, Crystallographic Computing, **Vol. 3**, Oxford University Press, Oxford, 1985, p. 175.